

Characteristics of HfO₂ thin films grown by plasma atomic layer deposition

Jinwoo Kim, Seokhoon Kim, and Hyeongtag Jeon^{a)}

Division of Materials Science and Engineering, Hanyang University, 133-791, Korea

M.-H. Cho and K.-B. Chung

Korea Research Institute of Standards and Science, Daejeon 305-600, Korea

Choelhwui Bae

Department of Physics, North Carolina State University, Raleigh, North Carolina 27695

(Received 28 February 2005; accepted 14 June 2005; published online 28 July 2005)

The characteristics of HfO₂ films grown on Si substrates using a tetrakis-diethyl-amino-hafnium precursor by the remote plasma atomic layer deposition (RPALD) and direct plasma ALD (DPALD) methods were investigated by physical and electrical measurement techniques. The as-deposited HfO₂ layer from RPALD exhibits an amorphous structure, while the HfO₂ layer from DPALD exhibits a clearly visible polycrystalline structure. Medium energy ion scattering measurement results indicate that the interfacial layer consists of the interfacial SiO_{2-x} and silicate layers. These results suggested that the stoichiometric change in the depth direction could be related to the energetic reactant in a state of plasma used in the plasma ALD process, resulting in damage to the Si surface and interactions between Hf and SiO_{2-x}. The as-deposited HfO₂ films using RPALD have the better interfacial layer characteristics than those using DPALD. A metal-oxide-semiconductor capacitor fabricated using the RPALD method exhibits electrical characteristics such as equivalent oxide thickness (EOT) of 1.8 nm with an effective fixed oxide charge density ($Q_{f,eff}$) of $\sim 4.2 \times 10^{11}$ q/cm² and that for DPALD has a EOT (2.0 nm), and $Q_{f,eff}$ ($\sim -1.2 \times 10^{13}$ q/cm²). © 2005 American Institute of Physics. [DOI: 10.1063/1.2005370]

Alternative gate dielectric insulators with high dielectric constants (high k) are in demand, because the aggressive scaling of Si metal-oxide-semiconductor (MOS) field effect transistors (FETs) limits the use of SiO₂ as a gate dielectric insulator.¹ Among the high- k materials that have been proposed to replace SiO₂ gate dielectrics, HfO₂ is one of the most promising candidates, due to its high dielectric constant ($k \sim 18$ – 25), wide band gap, and good thermal stability.²

Atomic layer deposition (ALD) has recently been widely studied for depositing high- k materials because the ALD process has many practical advantages, such as precise thickness control and uniform film properties.^{3–5} The ALD process, with halogen precursors, provides good step coverage and a low impurity concentration in thin films.^{6,7} However, several problems are associated with this method, such as the halogen atom residue in films, corrosion of gas delivery lines, and generation of particles. The ALD with metal organic precursors has been suggested to overcome these problems.⁸ Although the use of an organic precursor has many advantages in growing the films using the ALD method, some problems have been reported, such as the low film density and high impurity contamination.

To resolve these problems, the plasma-enhanced ALD (PEALD) method has been suggested to grow high- k thin films. The PEALD method is expected to increase the reactivity of the precursors, reduce impurities, widen the process window, and produce dense films. For the above reasons, PEALD appears to be the key next generation deposition technology for semiconductor devices.⁹ Although the PEALD method has many advantages for the deposition of high- k thin films, the effect of plasma damage on the depos-

ited high- k films and substrates has not been extensively studied.

In this letter, we applied both the remote plasma ALD (RPALD) and direct plasma ALD (DPALD) methods to the deposition of HfO₂ thin films. After deposition of the HfO₂ films by these two different PEALD methods, we investigated the physical, chemical, and electrical characteristics of HfO₂ gate dielectrics.

The HfO₂ thin films were deposited on p -type Si substrates with a $\langle 100 \rangle$ orientation and a resistivity of 6–12 Ω m. The HfO₂ films of about 5.0-nm-thick films were prepared at a substrate temperature of 250 °C. Prior to HfO₂ deposition, the Si substrates were cleaned in a diluted HF (1%) solution to remove native oxides and other residues. The hafnium precursor, tetrakis-diethyl-amino-hafnium (TDEAH), was introduced into the ALD chamber by a bubbler using argon as the carrier gas. The oxygen reactant was produced during the pulse of the O₂ plasma. The basic one cycle consists of supplying the hafnium precursor and oxygen plasma as a chemical source and a reactant gas, respectively. Argon purge gas was introduced for the complete separation of the precursor and reactant gas. Each deposition rate is approximately 1.0 Å/cycle with RPALD and 1.1 Å/cycle with DPALD at a deposition temperature of 250 °C.

The physical thickness of the films was determined by cross-sectional high-resolution transmission electron microscopy (HRTEM). The chemical composition and physical characteristics of the as-deposited HfO₂ film were analyzed by x-ray photoelectron spectroscopy (XPS) and medium energy ion scattering measurement (MEIS).¹⁰ The MOS capacitors were fabricated with a HfO₂ thickness of 5.0 nm and a Pt electrode thickness of 100 nm. For the post deposition annealing, the substrate was rapid-thermal annealed at 800 °C for 10 s in a N₂ atmosphere. A postmetallization an-

^{a)} Author to whom correspondence should be addressed; electronic mail: hjeon@hanyang.ac.kr

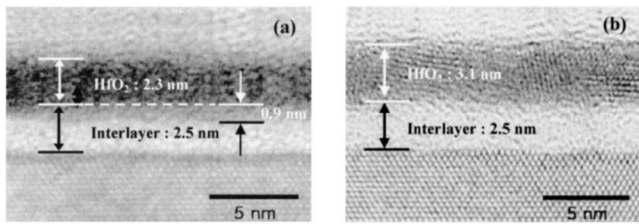


FIG. 1. Cross-sectional HRTEM images of as-grown HfO₂ films deposited on a Si substrate by (a) RPALD and (b) DPALD at a deposition temperature of 250 °C using Hf(NiEt₂)₄ precursor.

neal was carried out in a hydrogen and nitrogen mixed atmosphere at 450 °C for 30 min. The capacitance-voltage (*C-V*) characteristics of the HfO₂ MOS capacitors were measured by the Keithley 590 analyzer.

Figure 1 shows the HRTEM images of as-deposited HfO₂ samples prepared by (a) RPALD and (b) DPALD, respectively. Comparing the contrast in the images, the thickness of the interfacial layers in the samples was approximately the same, whereas the thickness of the DPALD HfO₂ layer (3.1 nm) without an interfacial layer was thicker than that of the RPALD HfO₂ layer (2.3 nm). The change in contrast in moving from the interfacial layer to the HfO₂ layer of the RPALD film was gradual, including the change in passing through the transition layer, whereas the contrast in the DPALD film changed abruptly when passing from the interfacial layer to the HfO₂ layer. In general, the interfacial reaction process depends on energetic species because it enhances the mixing of atoms and chemical reactions near the substrate by the momentum transfer and diffusion.¹¹ The thickness and stoichiometry of the interfacial layer were checked using MEIS, and will be discussed later. We also observed that the as-deposited RPALD HfO₂ layer was amorphous, whereas the as-deposited DPALD HfO₂ layer was polycrystalline. The HfO₂ thin film with a thickness of <5.0 nm grown using the ALD process without a plasma was reported to have an amorphous structure.¹⁰ However, in our DPALD films having a 3-nm-thick HfO₂ layer, the films became partially crystallized [as shown in Fig. 2(b)]. Metastable species in plasma were considered to release their energy through collisions, which resulted in the crystallization.¹¹ Therefore, we conclude that the crystallization of the DPALD sample is induced as the result of an enhanced physical reaction of oxygen ions. It has been suggested that the remote plasma ALD method minimizes the problems of direct plasma effects.

Figure 2 shows the chemical states of as-deposited HfO₂ samples investigated by XPS. A difference in the Hf 4*f*_{7/2} peak position between the RPALD and DPALD HfO₂ films, a lower bonded peak at the position of ~16.6 eV and a

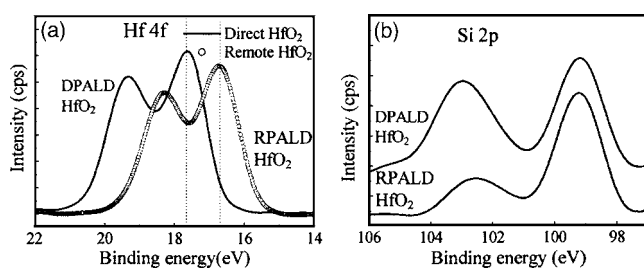


FIG. 2. XPS spectra of as-grown RPALD and DPALD HfO₂ films: (a) Hf 4*f* spectra and (b) Si 2*p* spectra of as-grown RPALD and DPALD HfO₂ film at 50 cycles at the plasma power of 100 W.

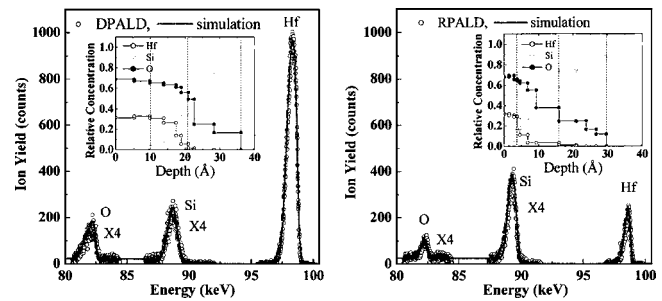


FIG. 3. MEIS results for as-grown DPALD (left) and RPALD (right) HfO₂ films: open circles and solid lines represent raw data and fitted data, respectively. The inset shows the calculated relative concentration in the depth direction of the films from the fitting results.

higher bonded peak at the position of 17.4 eV, were observed in Fig. 2(a). Wilk *et al.* reported that the Hf 4*f*_{7/2} peak of Hf silicate is ~1 eV higher than that of HfO₂, which is located at ~16.5–17 eV.¹² Thus, this peak shift to a higher binding energy for the DPALD sample indicates the formation of Hf silicate, indicating that the silicate formation is relatively increased compared to the RPALD sample. In Fig. 2(b), the Si 2*p* spectra also shows that the thickness and stoichiometry of the interfacial layers, including the Hf silicate layer of the two samples are not the same; i.e., the position and intensity with a higher binding energy, which results from the silicate and the SiO₂ layer, are not the same.

In order to investigate the stoichiometry in the interfacial layer and its layer thickness in the depth direction, MEIS measurements were carried out as shown in Fig. 3. The molecular density of HfO₂ (~2.49 × 10²² Hf atom/cm³) was used to extract the stoichiometry in depth direction from the MEIS data indicating the areal density. We prepared a HfO₂ film with a thickness of about 4 nm to examine the damage caused to the Si substrate by the plasma charge, and to determine the chemical stoichiometry of the interfacial layer. The spectrum of the Hf peak in two samples shows clear differences: i.e., using RPALD, the quantity of grown Hf is extremely small, compared to the sample prepared using DPALD. This difference in Hf quantity suggests that the growth rate of HfO₂ using DPALD is relatively higher than that of using RPALD. Since the amount of chemisorbed Hf at the first cycle is not totally dependent on the activity of the reactant in the case of ALD growth considering the steric hindrance factor containing the size effect of molecular bonded on substrate, the difference in growth rate can be related to newly generated active sites that are able to chemically react with TDEAH molecules. In general, an energetic reactant in a state of plasma results in a change of the surface

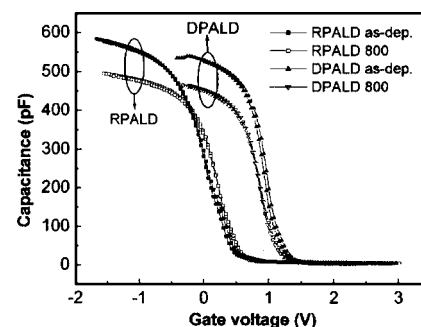


FIG. 4. Capacitance-voltage (*C-V*) curves for as-grown and annealed HfO₂ films deposited by RPALD and DPALD.

TABLE I. Summary of the electrical properties of HfO₂ films deposited by the RPALD and DPALD methods.

Film condition	Physical thickness	Hysteresis	C_{acc}	EOT	V_{fb}	$Q_{f,eff}$
	(nm)	(mV)	(pF/m ²)	(nm)	(V)	(q/cm ²)
RPALD-As	4.8	50	602	1.51	0.51	1.6×10^{12}
RPALD-800 °C	5.4	20	510	1.87	0.58	4.2×10^{11}
DPALD-As	5.6	120	543	1.60	1.33	-1.4×10^{13}
DPALD-800 °C	6.0	80	472	2.00	1.25	-1.2×10^{13}

state on Si, SiO_{2-x}, and HfO₂ to more active sites where the Hf source reacts during the Hf feeding period. It is also noteworthy that a difference in the stoichiometry of the interfacial layer in the depth direction is clearly observed between the two samples, as shown in the fitting data of the Fig. 3, represented by a solid line. The thickness of the interfacial layer, including O-deficient SiO_{2-x} and silicate, is almost the same in the two samples, while the stoichiometry of the silicate layer is very different. In addition, the thickness of the SiO_{2-x} layer in the DPALD is thicker than that of RPALD, while that of silicate layer in the DPALD is thinner than that of RPALD. Thus, a Hf-rich silicate layer is formed in the DPALD process, while a Si-rich silicate layer is produced in the RPALD process. This suggests that the stoichiometric change in the depth direction is related to the energetic reactant in a state of plasma, resulting in damage to the Si surface and interactions between Hf and SiO_{2-x}. Although the thickness observed using MEIS is not consistent with TEM because the used areal density of the film is not correct with the ideal value, the relative difference in thickness clearly reflects the differences between the two samples.

The quality of the interface and dielectric layer prepared by RPALD and DPALD was compared by fabricating MOS capacitors with a Pt top electrode. Figure 4 shows high frequency C - V curves measured at 1 MHz for these MOS capacitors before and after annealing at 800 °C. After annealing at 800 °C, the hysteresis of the RPALD sample and DPALD sample were ~ 20 and ~ 80 mV, respectively. For these capacitors, 10 mV corresponds to $\sim 1 \times 10^{11}$ q/cm². Table I summarizes the electrical properties of the MOS capacitors shown in Fig. 4. $Q_{f,eff}$ was calculated from $V_{fb} = \Phi_{ms} \pm Q_f / C_{acc}$, where Φ_{ms} is the difference in work function between the Pt electrode and the Si substrate, and C_{acc} is maximum accumulation capacitance. To determine Φ_{ms} in our MOS samples, the effective work function of Pt set at 5.6 V, and the doping concentration of p -type Si substrate was 5×10^{15} /cm². Then, Φ_{ms} (or ideal V_{fb}) is calculated to be 0.62 V.

The equivalent oxide thickness (EOT) for the RPALD sample was decreased compared to the samples using the direct plasma, resulting from a difference in film thickness, as shown in TEM and MEIS data. After annealing at 800 °C, the EOT for both samples was increased due to the decreased series capacitance of the increased interfacial layer. V_{fb} for the RPALD samples approached the ideal V_{fb} , 0.62 V more closely than that of the DPALD samples. After annealing at 800 °C, the V_{fb} for both samples were shifted in the direction of the ideal V_{fb} , 0.62 V. For the RPALD samples, $Q_{f,eff}$ decreased from 1.6×10^{12} to 4.2×10^{11} q/cm² as the result of the annealing process. For the DPALD samples, $Q_{f,eff}$ decreased from -1.4×10^{13} to -1.2×10^{13} q/cm². Yeo *et al.*

reported that the effective work function of Pt for Pt/HfO₂/Si structure was 5.3 V.¹³ In this case, the ideal V_{fb} for our MOS samples would be 0.32 V instead of the 0.62 V used in Table I. Using the ideal V_{fb} value, the C - V curves shown in Fig. 4 indicate a negative $Q_{f,eff}$ for all of the MOS samples. Nevertheless, the DPALD samples still had higher amount of negative true Q_f than the RPALD samples. These large amounts of negative fixed oxide charges of the DPALD samples represent the negative charging effects due to the direct plasma process.

In summary, we report here on an investigation of the effects of a remote plasma and direct plasma on the ALD process for HfO₂ thin films. The as-deposited HfO₂ layer from RPALD sample had a completely amorphous structure while a clearly visible polycrystalline structure was found for DPALD. The MEIS results indicate that the stoichiometric change in the depth direction could be related to the energetic reactant in a state of plasma used in the ALD process, resulting in damage to the Si surface and interactions between Hf and SiO_{2-x}. It has been suggested that the remote plasma ALD method minimizes the problems of direct plasma effects. The effective fixed oxide charge density is less for HfO₂ films deposited using RPALD than that for DPALD.

This study was supported by the National Program for Tera-level Nano-devices of the Ministry of Science and Technology as one of the 21st Century Frontier Programs.

¹G. D. Wilk, R. M. Wallace, and J. M. Anthony, *J. Appl. Phys.* **89**, 5243 (2001).

²G. D. Wilk, D. A. Muller, *Appl. Phys. Lett.* **83**, 3984 (2003), and reference therein.

³T. Suntola, *Handbook of Thin Film Process Technology*, 1st ed. (Institute of Physics, London, 1995), p. 71–81.

⁴M. Ritala, M. Leskela, E. Rauhala, and P. Haussalo, *J. Electrochem. Soc.* **142**, 2731 (1995).

⁵J. W. Uhm, S. S. Lee, J. W. Lee, T. H. Cha, K. S. Yi, Y. D. Kim, and H. Jeon, *J. Korean Phys. Soc.* **35**, 765 (1999).

⁶T. A. Pakkanen, V. Nevalainen, M. Lindbald, and P. Makkonen, *Surf. Sci.* **188**, 456 (1987).

⁷M. Ritala and M. Leskela, *Handbook of Thin Film Materials*, edited by H. S. Nalwa (Academic, San Diego, 2002), pp.103–113.

⁸H. K. Kim, J. Y. Kim, J. Y. Park, Y. Kim, W. M. Kim, Y. D. Kim, and H. Jeon, *J. Korean Phys. Soc.* **41**, 739 (2002).

⁹Sandy X. Lao, Ryan M. Martin, and Jane P. Chang, *J. Vac. Sci. Technol. A* **23**, 488 (2005).

¹⁰M.-H. Cho, Y. S. Roh, C. N. Whang, K. Jeong, S. W. Nahm, D.-H. Ko, J. H. Lee, N. I. Lee, and K. Fujihara, *Appl. Phys. Lett.* **81**, 472 (2002).

¹¹Alfred Grill, *Cold Plasma in Materials Fabrication* (Institute of Electrical and Electronics Engineers, New York, 1994), pp. 74–80.

¹²G. D. Wilk, R. M. Wallace, and J. M. Anthony, *J. Appl. Phys.* **87**, 484 (2000).

¹³Y.-C. Ye, Pushkar Ranade, T.-J. King, and Chenming Hu, *IEEE Electron Device Lett.* **23**, 342 (2002).